New Frontiers in Ophthalmology

Research Article

ISSN: 2397-2092

Selected aspects of retinal signaling and energy metabolism and its perspective as a cerebral surrogate model

Walid Albanna[1,2*], Jan Niklas Lüke[1], Serdar Alpdogan[1], Catharina Conzen[2], Miriam Weiss[2], Jürgen Hescheler[1], Hans Clusmann[2], Matthias Lüke[1], Gerrit Alexander Schubert[2] and Toni Schneider[1*]

[1]Institute for Neurophysiology, University of Cologne, Cologne, Germany

[2]Department of Neurosurgery, RWTH Aachen University Hospital, Germany

Abstract

Purpose: The isolated and superfused retina from vertebrates is routinely used for neurophysiological measurements of basic retinal signal generation and transduction. Such an ex vivo isolated neural network moreover represents a useful model system for the investigation of drugs and toxins and may also be helpful to elucidate molecular mechanisms of CNS diseases. The present overview aims to bring observations to the reader's attention, which, in part, have been made more than 50 years ago and were sparsely followed up upon in subsequent research, but may support the idea that the isolated bovine retina represents a useful system to investigate the physiology and pathophysiology of energy supply to neuronal tissue.

Material and methods: Parallel recording of ERGs and pyridine nucleotide oxidation in the isolated and superfused vertebrate retina. The review will focus on topics, which discuss the connection between retinal electrophysiology and underlying energy metabolism.

Results: Previous and present reports about (i) transretinal signaling cascades, (ii) the involvement of the pharmacoresistant Cav2.3 / R-type calcium channel in transretinal signaling and (iii) data about the retinal oxygen demands and concentration in different layers are collected, which elucidate that the retina may be used as a cerebral surrogate model in different research areas. Retinal tolerance to ischemia is several times larger than the tolerance in the remaining brain.

Conclusions: The retinal energy supply through retinal vessels is regulated and controlled by neurovascular coupling. Classical retinal recording techniques and special retinal abilities in electrical-vascular coupling will be set in perspective with novel recording techniques, currently brought into clinical application for the detection of impaired neurovascular coupling after aneurysmal subarachnoid hemorrhage in the brain. The present review elucidates that important pathophysiological aspects related to the upregulation of pharmacoresistant Cav2.3 / R-type calcium channels during SAH may be investigated in the isolated vertebrate retina.

Ischemic tolerance in the vertebrate retina

The oxygen consumption of the vertebrate retina on a per gram basis has been described as higher than that of the brain [1,2]. Oxygen cannot be "stored" in tissue so that a constant and adequate supply must be guaranteed to preserve function. Metabolic dysfunction regarding to impaired vascular supply is directly reflected by retinal oxygen saturation which can be detected noninvasively by dual wavelength fundus photography [3]. Normally, the oxygen saturation in retinal vessels differs along vascular segments and is higher in the macular region than retinal periphery [4]. Many retinal diseases are caused by a dysfunction of the vascular network. Interestingly, the venous oxygen saturation in diabetic retinopathy was higher in venules draining the macular surroundings than retinal periphery that reflect specific metabolic conditions [5, 6].

Since a relatively unobstructed light path to the photoreceptors is needed within the retina, the extent of vascularization within the retina itself is limited and varies in different regions of the same retina [7]. In the rat, under normal physiological conditions, intraretinal oxygen profiles show the highest oxygen tension (more than 40 mmHg) close to the deep choroid region, and the lowest oxygen tension (5-10 mmHg) within the retinal network. An intermediate elevation (15 – 20 mmHg) can be found close to the deep retinal capillary layer [8]. In highly energy consuming regions, the pO_2 may be demonstrated to be low, as it is around inner segments, or high, as it would be around ganglion cells that happen to be near a blood vessel. We believe, that additional vascularization is helpful for a better oxygen supply, as it is realized in mouse and man.

Although the vertebrate retina preserves a high metabolic rate, its tolerance to acute ischemia is several times larger than in the remaining brain [9], which may in part be related to a difference in glutamate release between retina and cerebral cortex following ischemia [10]. Furthermore, the activation of ATP-sensitive potassium channels in the retina plays an important role in the mechanism of preconditioning by enhancing the resistance of the retina against a severe ischemic insult [11]. In addition, the reprogramming of toll-like receptor 4 by brief ischemia or lipopolysaccharides (LPS) also contributes to better tolerance in retinal ischemia by microglia activation [12]. The

Correspondence to: Walid Albanna, Department of Neurosurgery, RWTH Aachen University, Pauwelsstr. 30, 52074 Aachen, Germany, Tel: +49 241 8036706; Fax: +49 241 8082420; E-mail: walbanna@ukaachen.de.

Toni Schneider, Institute of Neurophysiology, University of Cologne, Robert-Koch-Str. 39, D-50931 Köln, Germany, Tel: +49-221-4786968; Fax: +49-221-4786965; E-mail: toni.schneider@uni-koeln.de.

Key words*: Murine ERG, isolated vertebrate retina, energy demand under light stimuli, neurovascular coupling*

Received: April 07, 2018; **Accepted:** April 25, 2018; **Published:** April 28, 2018

preventive effects of LPS preconditioning revealed cell type-specificity of retinal cells. There was a complete rescue of ganglion cells, partial rescue of bipolar and photoreceptor cells or no rescue of amacrine cells, respectively. In healthy subjects, the difference in ischemia tolerance between the eye and the brain was investigated and proven by quantifying the time for visual alterations, peripheral light loss and blackout during and after self-induced retinal ischemia [13].

Parallel quantification of light-evoked signal transduction and oxygen consumption

Besides oxygen consumption, electrical responses are routinely recorded non-invasively from humans as ECG or EEG. Less well known is the recording of ERG-responses and oxygen consumption in parallel, which can be performed ex vivo in the isolated and superfused retina.

Ex vivo ERG recording and determination of pyridine nucleotide oxidation

Firstly in 1965, simultaneous respiratory and electrical responses to light stimulation were reported for the isolated and superfused frog retina, a poikilotherm organism [14]. While the isolated electrical recording from the ex vivo mammalian retina still had been successfully performed earlier [15], the use of absorption spectroscopy for measuring the energy status in parallel was indirectly introduced by Sickel [14]. The parallel recording of absorption changes for the oxidized versus reduced nicotinamide-adenine-dinucleotide had been developed by Chance and Williams [16] and was combined with ERG recordings by Sickel's systematic investigations in Boston and Cologne. He used frog retinas, which were isolated under dim red illumination and placed on a black plastic support separating two halves of the recording chamber. The nutrient solution perfused both halves of the chamber successively. Silver ring electrodes in both compartments served to record the ERG from the bathing fluid [14], a setup, which is still in use today in a modified form (Figures 1 and 2).

During the initial experiments in the 1960s, the retina was exposed to both an ultraviolet-analyzing and a visible-stimulating (and adapting) light beam. Single light flashes of one to several seconds or trains of 1-second stimuli with identical intervals of darkness were applied every 3 minutes. A 6 second light stimulus provoked a classical ERG response including a little rest of the visible negative deflecting a-wave and a prominent b-wave response. Concomitantly, the absorption of the UV beam decreased at the wave length of 350 nm (absorption maximum for NADH is at 340 nm). The reduction of absorption was even larger, when the light stimuli were given as a flickering light, which increased the energy demand. At that time, analogous absorption changes had been observed during induced physiological activity both in magnitude and direction in skeletal muscle [17]. This had been interpreted as oxidation of NADH via the redox partner from the mitochondrial electron transport chain with the resulting electron flow from the reduced NADH + H^+ to oxygen. The interpretation that the absorption changes at 340 / 350 nm represent the redox status of NAD/NADH + H^+ linked to metabolic reactions was supported by independent measurements of radiolabeled $^{14}CO_2$ released after feeding radiolabeled glucose. Under flickering light, the release of $^{14}CO_2$ increases, while the rate is reduced under longer lasting continuous light and increased during the consecutive dark adaptation period [18].

A normal metabolism based on a sufficient glucose (and oxygen) supply was shown by electroretinography to be crucial for proper transretinal signaling [19]. The b-wave amplitude as a measure for transretinal signaling was dependent on a normoglycemic glucose

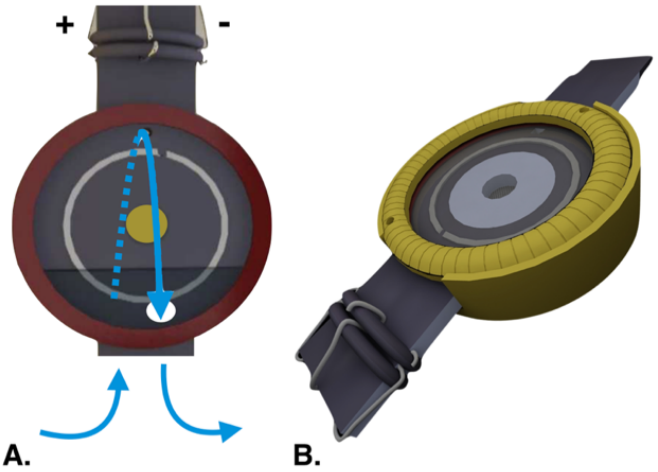

Figure 1. Recording chamber for the isolated and superfused retina [74].

A. Frontal view of the inner holder for the recording chamber. The retina is placed on a nylon mesh in the central hole of the holder (yellow circle), where it is held in place by an O-ring. The inner holder is then sealed by gaskets and glass plates and secured by the outer part of the recording chamber. To prevent formation of air bubbles in the inner holder and achieve complete superfusion of the retina from both sides, nutrient solution is supplied from the bottom, flows to the rear part of the chamber and reaches the other side through a small opening above the central hole (blue arrows). Electrical contact is provided by concentric Ag/AgCl electrodes located in the front and rear side of the inner holder (anode and cathode) and on the retinal plane between anode and cathode (reference electrode).

B. 3D illustration of the recording chamber when completely assembled.

supply of 5 mmol/l. Under glucose-free conditions, the b-wave was lost, while the a-wave, indicative for excitation generation, could still be recorded. Reperfusion of glucose reestablished the b-wave leading to a full ERG [19].

Superfusion of elevated glucose concentrations (15 mmol/l) initially decreased the b-wave amplitude. When the hyperglycemic concentration was reduced to zero, the b-wave amplitude increased after a delay of about 15 minutes. In parallel, the oxidation of NADH was accelerated (recorded as a decrease of UV-absorption at 350 nm [Figure 3 in Sickel, 1968] [19]. In summary, these early investigations of the light effect on retinal energy metabolism lead to 3 conclusions [20]: (i) A depression of oxygen uptake or CO_2-output for the duration of the light exposure. (ii) Transitory increases of the energy metabolism during repetitive changes of light intensity, increasing or decreasing (flickering light). (iii) An oxygen debt accruing from prolonged quantum catch. Obviously, the retina represents a sensory system with high energy demand. Repetitive light intensity changes can be easily used to increase the energy metabolism.

Quantification of required oxygen and effects of electron transport inhibitors and uncouplers

Interestingly, under dark adaptation conditions a quantitative estimate was made for the oxygen needed during neural processing of a just saturating brief light flash, which requires approximately 300 pmoles of oxygen per mg dry weight of retina. It corresponds to an amount of energy several million-fold larger than that amount of the quanta absorbed with a single flash [20]. In 1994 it was reported that these early parallel recordings of electric field potential changes, and the absorption changes of the pyridine nucleotides may not have been taken up by the scientific readership, so that new data were measured and published carefully extending and proving the correlation between ERG-parameters and optical response at 350 nm [21].

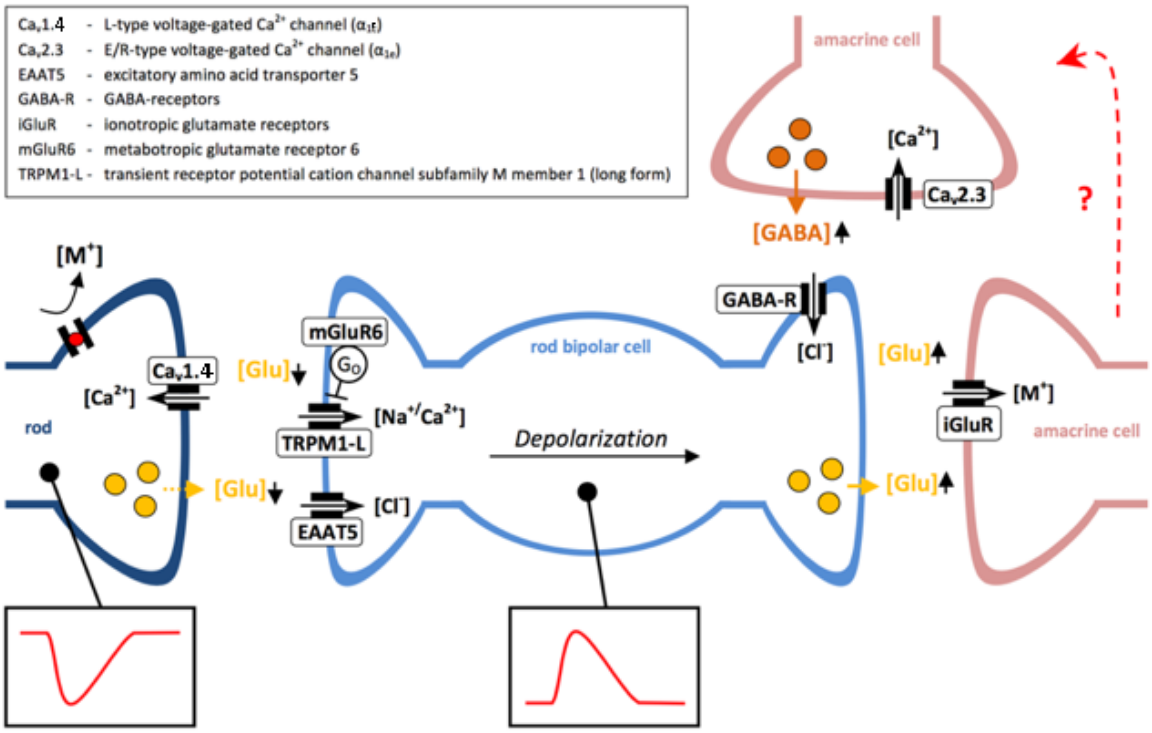

Figure 2. Schematic representation of signal transduction through rod bipolar cells.

Light stimulation hyperpolarizes rod photoreceptors, leading to decreased glutamate release and depolarization of rod bipolar cells. Rod bipolar cells excite amacrine cells, which synapse on to ON or OFF bipolar cells of the cone pathway (not shown). In addition, amacrine cells are involved in reciprocal inhibitory pathways, which modulate rod bipolar cell depolarization via GABAergic projections. Although the exact circuits remain to be elucidated, there is evidence that Ca$_v$2.3 channels may be involved in GABAergic reciprocal inhibition. [M$^+$] = non-selective cations.

A more detailed analysis followed and included the perfusion of electron transport inhibitors and uncouplers of the mitochondrial proton gradient aside from the effects of oxygen and glucose withdrawal [22]. Different energetic states could be demonstrated under the conditions selected. Superfusing the isolated frog retina in the dark with a medium containing sufficient oxygen (saturated) and glucose (5 mmol/l) led to the resting state 4, characterized by a low respiration rate and a low amount of adenosine diphosphate (ADP). The starved state 2 could be simulated by the withdrawal of glucose from the medium leading to an increase in overall transmission at 350 nm, which represents a slow transition of the NADH/NAD ratio towards the oxidized form [22]. Disturbances in the mitochondrial energy metabolism may be a major risk factor during neurodegeneration. The authors conclude that future research will help to elucidate the underlying mechanisms leading to retinal neurodegeneration as the age-related macular disease.

Constant and flickering light affect retinal metabolism differently. Under constant light, as opposed to darkness, retinal metabolism has been reported to be reduced (for an overview see Wang *et al.* 1997 [23]). The effect of light on retinal metabolism in the inner and outer retina is different. Steady and / or flicker light have the same metabolic effect on photoreceptors as long as the time averaged illumination is the same and it is only in the inner retina where flicker has a bigger effect on metabolism [24].

In contrast, flickering light stimulates glucose consumption not only in the amphibian but also in the primate retina, and increases retinal blood flow [25,26] and lactate formation [2]. Besides, catabolic vascularization and metabolism vary between species, for instance, rabbits are not good models for the inner retina of higher animals, because their metabolism is entirely glycolytic, and while the same principles apply to photoreceptor metabolism in poikilotherms and homeotherms, there are substantial quantitative differences.

The importance of retinal glucose supply was reconfirmed more recently in mice and compared within mitochondria from different mouse retina-mutants. Also in mice, similar as in frogs, inhibitors of the mitochondrial electron transport chain as well as uncouplers of the mitochondrial proton gradient changed the oxygen consumption rate confirming the high vulnerability of photoreceptors to altered energy homeostasis in mice [27].

Neurovascular coupling and the use of the vertebrate retina as a model system

As an extension of the brain, the eye contains a highly organized neuronal network which may be used for noninvasive investigation and early diagnosis of CNS disorders such as stroke [28], multiple sclerosis [29], Parkinson disease [30] and Alzheimer disease [31]. The vertebrate retina represents also a valuable model to study signaling from the neuronal network to the microvascular system, which is responsible for the energy supply via the blood circulation. The retina contains neurons, which are well organized in a network with reciprocal coupling for signal transduction at extreme different light intensities (see chapter 3.3 for more details). On the other hand, the isolated murine retina contains retinal arterioles and venules with similar features as small cerebral blood vessels with auto-regulative function. Even more so, retinal microvascular changes may reflect similar pathophysiological processes as in the cerebral microvasculature [32]. Indeed, retinal vessel

analysis in humans is technically feasible in patients with subarachnoid hemorrhage and can detect fluctuations in vessel diameter and its autoregulatory characteristics [33].

Pathophysiology of subarachnoid hemorrhage

Recent reviews have summarized the present understanding of the pathophysiology of aneurysmal subarachnoid hemorrhage (SAH) quite in detail [34,35]. In most patients, the reason for spontaneous SAH arises from cerebral aneurysm rupture [36]. The pathophysiological processes following SAH may cause severe impairment for the survivors with significant mortality and morbidity.

Within the course of SAH two phases are distinguished: within the first three days the initial pathophysiological changes are summarized as "early brain injury" (EBI). Angiographic vasospasm associated with delayed cerebral ischemia (DCI) can occur in the subsequent phase (classically day 4-14) causing severe neurological restrictions to the preinjured brain. The underlying mechanisms are multifactorial and not yet fully understood, one major mechanism includes microvascular dysfunction. Up to 70% of all arterioles are affected during microvascular spasms. They are thought to originate from exposure to blood components, particularly oxygenated hemoglobin and partially by blood degradation products such as bilirubin and its oxidation endproducts (BOXes) [35]. Aside from that, a set of typical pathophysiological mechanisms contributes to DCI including microvascular dysfunction, microthrombosis, cortical spreading depolarization and inflammation reactions. In the current understanding, they go far beyond angiographic vasospasm of the major cerebral vessels and additionally contribute to neuronal ischemia.

Many factors are known to regulate cerebral blood flow, and the precise physiological conditions, under which these molecules induce changes in the vessel diameter, are not yet fully understood. However, recent studies have shown that astrocytes are critical players in the regulation of cerebral blood vessel diameter for the purpose of adapted metabolism [37]. Astrocytes may act as sensors of neuronal activity and metabolism to coordinate the transport and delivery of nutrients and oxygen via the blood to metabolically active cells [38]. They are able to act bidirectional, causing either vasoconstriction or vasodilatation. For both vasomotor responses arachidonic acid is synthetized by the Ca^{2+} sensitive phospholipase A_2. For vasoconstriction, arachidonic acid is converted to 20-hydroxyeicosatetraenoic acid, and for vasodilatation, it is converted to epoxyeicosatrienoic acid or prostaglandins. Several factors determine the direction of action, including brain oxygen, lactate, adenosine as well as nitric oxide [38].

Within the neurovascular unit (neurons – astrocytes – parenchymal arterioles), the neurovascular coupling adopts the local blood flow to the current neuronal activity. Under normal conditions, parenchymal arterioles may dilate and constrict according to metabolic demand in normophysiologic control compartments in the brain. After aneurysmal subarachnoid hemorrhage (aSAH), neurovascular coupling is inverted [39]. The vasoconstriction observed after SAH is thought to be caused by elevated potassium concentrations outside ($[K^+]_o$) the cells. It is likely that the increased spontaneous astrocytic Ca^{2+} oscillations activate endfoot large-conductance Ca^{2+}-activated potassium channels leading to a lower increase of $[K^+]_o$ in an restricted perivascular space [39]. Such an inversion of neurovascular coupling has also been demonstrated in vivo [40,41].

Voltage-gated ion channels of the retina may be involved in SAH

The signaling cascade during neurovascular coupling which is evidently disturbed during angiographic vasospasm, should include up- or downregulated voltage-gated ion channels in addition to the mentioned Ca^{2+}-activated K^+ channels as well as less well investigated signaling components. Much is known about the beneficial effects of dihydropyridine L-type calcium (Ca^{2+}) channel antagonists that are routinely recommended in clinical practice for the prevention and treatment of DCI [34]. When applied in a rather high local concentration, side effects on additional voltage-gated Ca^{2+} channels may be assumed, which are rather up- than downregulated in experimentally induced SAH in dogs [42]. For $Ca_v2.3$ (R-type) Ca^{2+} channels it is established that their expression and current density is increased in rabbit cerebral artery myocytes [43,44]. Similar results were found for two out of three T-type (transiently and low voltage-activated Ca^{2+} channels), named $Ca_v3.1$ and $Ca_v3.3$ [42]. The retina as an organotypical neuronal network expresses several voltage-gated calcium channels ($Ca_v1.2$, $Ca_v1.3$, and $Ca_v1.4$), and R-type calcium channel $Ca_v2.3$. The retina also contains T-type calcium channels, which were also considered to be involved in the mechanism of experimentally induced aSAH, too [42,45].

Transretinal signaling of neuronal networks

In the past, the model of the isolated and superfused vertebrate retina was frequently used for the screening of drug and other toxin effects on the sensitive phototransduction and transretinal signaling [20,46-48]. Frog, bovine and murine retinas have proven to represent a valuable neuronal network including transretinal signaling via L-type, T-type and R-type voltage-gated Ca^{2+} channels. They constitute different parts of the ERG. The major L-type voltage-gated Ca^{2+} channel at the photoreceptor synapses is $Ca_v1.4$ in both retinal rods and cones [49]. T-type currents have been recorded in retinal bipolar cells [50]. The function of the $Ca_v2.3$/R-type Ca^{2+} channel is related to reciprocal inhibition of bipolar cell signaling (Figure 2).

The sensitivity towards bipolar cations was used to unravel its function during transretinal signaling. Transient effects of micromolar / submillimolar Ni^{2+} concentrations had earlier been recorded for the frog retina [51]. Low concentrations (10 and 30 μM) augmented the b-wave amplitude while higher concentrations (100 μM) inhibited the b-wave amplitude reversibly. Starting from this observation, our group repeated the experiments for the bovine [52] and the murine retina [53]. Isolated murine retinas from control mice and from $Ca_v2.3$-deficient (as well as from Cav3.2/T-type-deficient) channels were compared for their response to 15 μM $NiCl_2$. It was concluded that $Ca_v2.3$ voltage-gated Ca^{2+} channels contribute to the reciprocal inhibitory control during transretinal signaling. The cell type in which $Ca_v2.3$ should be expressed, was assumed but not proven to be a subtype of amacrine cells. However, it is not excluded that other neurons or even glial cells may harbor the $Ca_v2.3$/R-type channel.

In the vascularized mammalian retina, spreading depolarization can also be demonstrated *in vivo* [54], which implies that voltage-(and ligand-)gated ion channels are involved in the surface spreading and must be altered in their activity in the retina as well. As the so called "pharmacoresistent" $Ca_v2.3$/R-type Ca^{2+} channel is expressed in the retina [55,56] and was found to be sensitive towards micromolar dihydropyridine concentrations [57,58], the isolated retina should be selected for investigating the molecular mechanisms of electric signaling during early and late stages of SAH, a disease, which is known to be worsened in outcome by a disturbed, maybe even by an inversed neurovascular coupling during which the vessels are constricted instead of being relaxed. For the isolated murine retina, the effect of blood degradation products on transretinal signaling can be investigated, and different murine genotypes can be used for the investigations to test for those targets which may be influenced by blood degradation products.

Conclusion and perspectives

The retina highlights a sensory system with enormous energy demand. As an embryologic part of the brain, the retina represents an organized neuronal network for early diagnosis of CNS diseases. We believe that the retina still deserves more observation through non-invasive technical tools in the future.

Acknowledgments

We would like to specially thank Mrs. Renate Clemens for her dedication and hard work.

Funding

This research program is supported by the START-Program of the Faculty of Medicine, RWTH Aachen, Germany.

References

1. Anderson B Jr, Saltzman HA (1964) Retinal oxygen utilization measured by hyperbaric blackout. *Arch Ophthalmol* 72: 792-795. [Crossref]
2. Ames A 3rd1, Li YY, Heher EC, Kimble CR (1992) Energy metabolism of rabbit retina as related to function: high cost of Na+ transport. *J Neurosci* 12: 840-853. [Crossref]
3. Hardarson SH, Harris A, Karlsson RA, Halldorsson GH, Kagemann L, et al. (2006) Automatic retinal oximetry. *Invest Ophthalmol Vis Sci* 47: 5011-5016. [Crossref]
4. Jani PD, Mwanza JC, Billow KB, Waters AM, Moyer S, et al. (2014) Normative values and predictors of retinal oxygen saturation. *Retina* 34: 394-401. [Crossref]
5. Jorgensen CM, Hardarson SH, Bek T (2014) The oxygen saturation in retinal vessels from diabetic patients depends on the severity and type of vision-threatening retinopathy. *Acta Ophthalmol* 92: 34-39. [Crossref]
6. Jorgensen CM, Bek T (2017) Lack of differences in the regional variation of oxygen saturation in larger retinal vessels in diabetic maculopathy and proliferative diabetic retinopathy. *Br J Ophthalmo* 101: 752-757. [Crossref]
7. Chase J (1982) The evolution of retinal vascularization in mammals. A comparison of vascular and avascular retinae. *Ophthalmology* 89: 1518-1525. [Crossref]
8. Yu DY, Cringle SJ (2001) Oxygen distribution and consumption within the retina in vascularised and avascular retinas and in animal models of retinal disease. *Prog Retin Eye Res* 20: 175-208. [Crossref]
9. Hayreh SS, Weingeist TA (1980) Experimental occlusion of the central artery of the retina. IV: Retinal tolerance time to acute ischaemia. *Br J Ophthalmol* 64: 818-825. [Crossref]
10. Iijima T, Iijima C, Iwao Y, Sankawa H (2000) Difference in glutamate release between retina and cerebral cortex following ischemia. *Neurochem Int* 36: 221-224. [Crossref]
11. Ettaiche M, Heurteaux C, Blondeau N, Borsotto M, Tinel N, et al. (2001) ATP-sensitive potassium channels (K(ATP)) in retina: a key role for delayed ischemic tolerance. *Brain Res* 890: 118-129. [Crossref]
12. Halder SK, Matsunaga H, Ishii KJ, Akira S, Miyake K, et al. (2013) Retinal cell type-specific prevention of ischemia-induced damages by LPS-TLR4 signaling through microglia. *J Neurochem* 126: 243-260. [Crossref]
13. Whinnery T, Forster EM (2015) Neurologic state transitions in the eye and brain: kinetics of loss and recovery of vision and consciousness. *Vis Neurosci* 32: E008. [Crossref]
14. Sickel W (1965) Respiratory and electrical responses to light simulation in the retina of the frog. *Science* 148: 648-651. [Crossref]
15. Ames A 3rd, Gurian BS (1963) Electrical recordings from isolated mammalian retina mounted as a membrane. *Arch Ophthalmol* 70: 837-841. [Crossref]
16. Chance B, Williams GR (1956) The respiratory chain and oxidative phosphorylation. *Adv Enzymol Relat Subj Biochem* 17: 65-134. [Crossref]
17. Connelly CM (1954) Kinetics of reduced pyridine nucleotides in stimulated frog muscle and nerve. *Federation Proceedings of the Am Physiol Soc* 13: 29.
18. Sickel W (1966) The isolated retina maintained in a circulating medium; combined optical and electrical investigations of metabolic aspects of generation of the electroretinogram. In: Clinical Electroretinography. *Supplement to Vision Research* pp 115-124. Oxford & New York: Pergamon Press.
19. Sickel W (1968) Retinal Oxidation-Reduction States. Effects of Varied Glucose Concentration on Resting Potential and Electroretinogram in the Perfused Frog's Retina. The Clinical Value of Electroretinography, *ISCERG Symp Ghent* 1966: 232-242.
20. Sickel W (1972) Electrical and metabolic manifestations of receptor and higher-order neuron activity in vertebrate retina. *Adv Exp Med Biol* 24: 101-118. [Crossref]
21. Walter P, Sickel W (1994) Identification of fast spurts of pyridine nucleotide oxidation evoked by light stimulation in the isolated perfused vertebrate retina. *Graefes Arch Clin Exp Ophthalmol* 232: 318-323. [Crossref]
22. Walter P, Alteheld N, Huth J, Roessler G, Vobig MA (2007) Different states of energy metabolism in the vertebrate retina can be identified by stimulus-related changes in near UV transmission. *Graefes Arch Clin Exp Ophthalmol* 245: 547-554. [Crossref]
23. Wang L, Bill A (1997) Effects of constant and flickering light on retinal metabolism in rabbits. *Acta Ophthalmol Scand* 75: 227-231. [Crossref]
24. Bill A, Sperber GO (1990) Aspects of oxygen and glucose consumption in the retina: effects of high intraocular pressure and light. *Graefes Arch Clin Exp Ophthalmol* 228: 124-127. [Crossref]
25. Bill A, Sperber GO (1990) Control of retinal and choroidal blood flow. *Eye (Lond)* 4: 319-325. [Crossref]
26. Riva CE, Logean E, Falsini B (2005) Visually evoked hemodynamical response and assessment of neurovascular coupling in the optic nerve and retina. *Prog Retin Eye Res* 24: 183-215. [Crossref]
27. Kooragayala K, Gotoh N, Cogliati T, Nellissery J, Kaden TR, et al. (2015) Quantification of Oxygen Consumption in Retina Ex Vivo Demonstrates Limited Reserve Capacity of Photoreceptor Mitochondria. *Invest Ophthalmol Vis Sci* 56: 8428-8436. [Crossref]
28. Smith W, Malan NT, Schutte AE, Schutte R, Mc Mels C, et al. (2016) Retinal vessel caliber and its relationship with nocturnal blood pressure dipping status: the SABPA study. *Hypertens Res* 39: 730-736. [Crossref]
29. Bhaduri B, Nolan RM, Shelton RL, Pilutti LA, Motl RW, et al. (2016) Detection of retinal blood vessel changes in multiple sclerosis with optical coherence tomography. *Biomed Opt Express* 7: 2321-2330. [Crossref]
30. Schneider JS, Ault ME, Anderson DW (2014) Retinal pathology detected by optical coherence tomography in an animal model of Parkinson's disease. *Mov Disord* 29: 1547-1551. [Crossref]
31. Einarsdottir AB, Hardarson SH, Kristjansdottir JV, Bragason DT, Snaedal J, et al. (2016) Retinal oximetry imaging in Alzheimer's disease. *J Alzheimers Dis* 49: 79-83. [Crossref]
32. London A, Benhar I, Schwartz M (2013) The retina as a window to the brain-from eye research to CNS disorders. *Nat Rev Neurol* 9: 44-53. [Crossref]
33. Albanna W, Conzen C, Weiss M, Clusmann H, Fuest M, et al. (2016) Retinal Vessel Analysis (RVA) in the Context of Subarachnoid Hemorrhage - A Proof of Concept Study. *PLoS One* 11: e0158781. [Crossref]
34. Tso MK, Macdonald RL (2014) Subarachnoid hemorrhage: a review of experimental studies on the microcirculation and the neurovascular unit. *Transl Stroke Res* 5: 174-189. [Crossref]
35. van Lieshout JH, Dibué-Adjei M, Cornelius JF, Slotty PJ, Schneider T, et al. (2017) An introduction to the pathophysiology of aneurysmal subarachnoid hemorrhage. *Neurosurg Rev.* [Crossref]
36. Van Gijn J, Kerr RS, Rinkel GJ (2007) Subarachnoid haemorrhage. *Lancet* 369: 306-318. [Crossref]
37. Gordon GR, Mulligan SJ, MacVicar BA (2007) Astrocyte control of the cerebrovasculature. *Glia* 55: 1214-1221. [Crossref]
38. Gordon GR, Howarth C, MacVicar BA (2016) Bidirectional Control of Blood Flow by Astrocytes: A Role for Tissue Oxygen and Other Metabolic Factors. *Adv Exp Med Biol* 903: 209-219. [Crossref]
39. Koide M, Bonev AD, Nelson MT, Wellman GC (2012) Inversion of neurovascular coupling by subarachnoid blood depends on large-conductance Ca2+-activated K+ (BK) channels. *Proc Natl Acad Sci U S A* 109: E1387-1395. [Crossref]
40. Balbi M, Koide M, Wellman GC, Plesnila N (2017) Inversion of neurovascular coupling after subarachnoid hemorrhage in vivo. *J Cereb Blood Flow Metab* 37: 3625-3634. [Crossref]
41. Balbi M, Koide M, Schwarzmaier SM, Wellman GC, Plesnila N (2017) Acute changes in neurovascular reactivity after subarachnoid hemorrhage in vivo. *J Cereb Blood Flow Metab* 37: 178-187. [Crossref]

42. Nikitina E, Zhang ZD, Kawashima A, Jahromi BS, Bouryi VA, et al. (2007) Voltage-dependent calcium channels of dog basilar artery. *J Physiol* 580. [Crossref]

43. Ishiguro M, Wellman TL, Honda A, Russell SR, Tranmer BI (2005) Emergence of a R-type Ca2+ channel (CaV 2.3) contributes to cerebral artery constriction after subarachnoid hemorrhage. *Circ Res* 96: 419-426. [Crossref]

44. Ishiguro M, Wellman GC (2008) Cellular basis of vasospasm: role of small diameter arteries and voltage-dependent Ca2+ channels. *Acta Neurochir Suppl* 104: 95-98. [Crossref]

45. Nikitina E, Zhang ZD, Kawashima A, Jahromi BS, Bouryi VA, et al. (2007) Voltage-dependent calcium channels of dog basilar artery. *J Physiol* 580: 523-541. [Crossref]

46. Lüke M, Weiergräber M, Brand C, Siapich SA, Banat M, et al. (2005) The isolated perfused bovine retina--a sensitive tool for pharmacological research on retinal function. *Brain Res Brain Res Protoc* 16: 27-36. [Crossref]

47. Albanna W, Banat M, Albanna N, Alnawaiseh M, Siapich SA, et al. (2009) Longer lasting electroretinographic recordings from the isolated and superfused murine retina. *Graefes Arch Clin Exp Ophthalmol* 247: 1339-1352. [Crossref]

48. Alnawaiseh M, Albanna W, Banat M, Abumuaileq R, Hescheler J, et al. (2011) Electroretinographic Recordings from the Isolated and Superfused Murine Retina. Belulsic G ed. Croatia: Electroretinograms.

49. Joiner ML, Lee A (2015) Voltage-Gated Cav1 Channels in Disorders of Vision and Hearing. *Curr Mol Pharmacol* 8: 143-148. [Crossref]

50. Hu C, Bi A, Pan ZH (2009) Differential expression of three T-type calcium channels in retinal bipolar cells in rats. *Vis Neurosci* 26: 177-187. [Crossref]

51. Sickel W (1976) Experimentelle Elektroretinographie der Metallosen. In: Intraokularer Fremdkörper und Metallose. Internationales Symposion der Deutschen Ophthalmologischen Gesellschaft (30.03.-02.04.1976 in Köln) (Neubauer H, Rüssmann W, Kilp H, eds), pp 111-118. München: J.F. Bergmann-Verlag.

52. Lüke M, Henry M, Lingohr T, Maghsoodian M, Hescheler J, et al. (2005) A Ni(2+)-sensitive component of the ERG b-wave from the isolated bovine retina is related to E-type voltage-gated Ca(2+) channels. *Graefes Arch Clin Exp Ophthalmol* 243: 933-941. [Crossref]

53. Alnawaiseh M, Albanna W, Chen CC (2011) Two separate Ni(2+) -sensitive voltage-gated Ca(2+) channels modulate transretinal signalling in the isolated murine retina. *Acta Ophthalmol* b;89: e579-590.

54. Srienc AI, Biesecker KR, Shimoda AM, Kur J, Newman EA (2016) Ischemia-induced spreading depolarization in the retina. *J Cereb Blood Flow Metab* 36: 1579-1591. [Crossref]

55. Kamphuis W, Hendriksen H (1998) Expression patterns of voltage-dependent calcium channel alpha 1 subunits (alpha 1A-alpha 1E) mRNA in rat retina. *Brain Res Mol Brain Res* 55: 209-220. [Crossref]

56. Xu HP, Zhao JW, Yang XL (2002) Expression of voltage-dependent calcium channel subunits in the rat retina. *Neurosci Lett* 329: 297-300. [Crossref]

57. Stephens GJ, Page KM, Burley JR, Berrow NS, Dolphin AC (1997) Functional expression of rat brain cloned alpha1E calcium channels in COS-7 cells. *Pflugers Arch* 433: 523-532. [Crossref]

58. Lu ZJ, Pereverzev A, Liu HL, Weiergräber M, Henry M, et al. (2004) Arrhythmia in isolated prenatal hearts after ablation of the Cav2.3 (alpha1E) subunit of voltage-gated Ca2+ channels. *Cell Physiol Biochem* 14: 11-22. [Crossref]

Copyright: ©2018 Albanna W. This is an open-access article distributed under the terms of the Creative Commons Attribution License, which permits unrestricted use, distribution, and reproduction in any medium, provided the original author and source are credited.